Coupled Activation of the Donor and the Acceptor Side of Photosystem II during Photoactivation of the Oxygen Evolving Cluster†

Maria Rova,‡,§ Fikret Mamedov,‡ Ann Magnuson,‡ Per-Olof Fredriksson,§ and Stenbjörn Styring*,‡

Department of Biochemistry, Chemical Center, Lund University, Box 124, S-221 00 Lund, Sweden, and Department of Chemistry, University of Karlstad, S-651 88 Karlstad, Sweden

Received February 18, 1998; Revised Manuscript Received April 8, 1998

ABSTRACT: Photoactivation of photosystem II has been studied in the FUD 39 mutant of *Chlamydomonas reinhardtii* that lacks the 23 kDa extrinsic subunit of photosystem II. We have taken advantage of the slow photoactivation rate of FUD 39, earlier demonstrated in Rova, E. M., et al. [(1996) *J. Biol. Chem.* 271, 28918−28924], to study events in photosystem II during intermediate stages of the process. By measuring the EPR multiline signal, the decay of the variable fluorescence after single flashes, and electron transfer from water to the Q_B site, we found a good correlation between the building of a tetrameric Mn cluster, longer recombination times between Q_A^- and the donor side of photosystem II, and the achievement of water splitting ability. An increased rate of electron transfer from Q_A^- to the Q_B site on the acceptor side of photosystem II, mainly due to enhanced efficiency of binding of Q_B to its site, was found to precede the building of the Mn cluster. We also showed that Tyr_D was oxidized simultaneously with this increase in electron-transfer rate. Thus, it appears that photoactivation is sequential, with an increased rate of electron transfer on the acceptor side occurring together with the oxidation of Tyr_D in the first step, followed by the assembly of the Mn cluster. We suggest that a conformational change of photosystem II is induced early in the photoactivation process facilitating electron transfer from the primary donor to the acceptor side. As a consequence, Tyr_D, an auxiliary electron donor to $P_{680}^+/Tyr_Z^\bullet$, is oxidized. That this occurs before the Mn cluster is fully functional serves to protect photosystem II against donor side induced photodamage.

Photosystem II (PS II)[1] is a large multisubunit complex that catalyzes the light-driven oxidation of water in plants, green algae, and cyanobacteria (*1*, *2*). The primary photochemical reaction in PS II produces the $P_{680}^+Pheo^-$ radical pair. This charge separation is stabilized by reduction of the primary plastoquinone electron acceptor, Q_A, on the acceptor side and by oxidation of a tyrosine residue in the D1 protein, Tyr_Z, which abstracts electrons from water molecules on the donor side of PS II.

Q_A^- reduces the secondary plastoquinone electron acceptor, Q_B, first to the semiquinone and after another charge separation to the quinol form. When Q_B is fully reduced, it leaves its site on the D1 protein as Q_BH_2, and the empty site is reoccupied by another quinone molecule from the plastoquinone pool. If this forward reaction is inhibited, a recombination reaction between Q_A^- or Q_B^- and oxidized species on the donor side (i.e., the Mn cluster, $Tyr_Z^\bullet$, or P_{680}^+) occurs.

To achieve water splitting, oxidizing power is stored in the water oxidizing center which contains a $(Mn)_4$ cluster that cycles through five different redox states, the S-states (S_0 to S_4) (*3*, *4*). When the PS II complex is assembled, the Mn cluster is created in a light-dependent process known as photoactivation. This process has been shown to be a low quantum yield process comprising two independent photoacts spaced by a dark period (*5*, *6*). Each photoevent probably corresponds to the oxidation of a Mn^{2+} ion (*7*, *8*) which leads to a stronger binding of the ion to the protein matrix. After the two photoacts, two more Mn ions bind in a light-independent way to form the tetrameric Mn cluster. For maximal water oxidizing capacity, the cofactors Ca^{2+} and Cl^- are needed, and they are thought to be essential also for the photoactivation process (*9*−*12*).

During photoactivation, highly oxidizing species such as P_{680}^+ and $Tyr_Z^\bullet$ are formed. This is a potentially dangerous

† This work was supported by the Swedish Natural Science Research Council, the Knut and Alice Wallenberg Foundation, and the Crafoord Foundation. A.M. gratefully acknowledges support by the Nordic Energy Research Program

* To whom correspondence should be addressed. Telephone: +46 46 222 0108. Fax: +46 46 222 4534. E-mail: stenbjorn.styring@biokem.lu.se.

‡ Lund University.

§ University of Karlstad.

[1] Abbreviations: Chl, chlorophyll; cyt b_{559}, cytochrome b_{559}; D1, one of the PS II reaction center proteins carrying some of the redox components in the electron transport chain through photosystem II; D2, the other redox component carrying protein of the reaction center; DCMU, 3-(3,4-dichlorophenyl)-1,1-dimethylurea; DCPIP, 2,6-dichlorophenolindophenol; DPC, 2,2′-diphenylcarbonic dihydrazide; E, einstein(s); EDTA, ethylenediaminetetraacetate; EPR, electron paramagnetic resonance; FUD 39, mutant strain of *C. reinhardtii* lacking the 23 kDa extrinsic subunit of PS II; Fv and Fo, variable and constant fluorescence respectively; HEPES, 4-(2-hydroxyethyl)-1-piperazineethanesulfonic acid; P_{680}, primary electron donor chlorophyll(s) of photosystem II; Pheo, pheophytin; PS II, photosystem II; Q_A, first quinone acceptor in photosystem II; Q_B, second quinone acceptor in photosystem II; Tris, tris(hydroxymethyl)aminomethane; Tyr_D, the redox active tyrosine residue on the D2 reaction center protein; Tyr_Z, the redox active tyrosine residue on the D1 reaction center protein.

S0006-2960(98)00381-X CCC: $15.00
Published on Web 07/17/1998

situation for a PS II complex without an assembled Mn cluster since it might lead to damages and degradation due to reactions with the oxidizing radicals, so-called donor side photoinhibition [for reviews, see (*13*−*15*)]. Ways to protect PS II from photoinhibition during the assembly of the Mn cluster have to exist, but our knowledge of those processes is scarce. It is, however, known that in a Mn-deficient PS II, P_{680}^+ can be rereduced by at least three alternative pathways: (i) by cyt b_{559} which was shown to be photooxidized by P_{680}^+ via a chlorophyll (*16*); (ii) by the second redox active tyrosine in PS II, Tyr_D, whose function is not clear; or (iii) by recombination with the reduced acceptor side.

Here, we have studied the photoactivation process in order to get more information on which reactions accompany the assembly of the Mn cluster. We have compared intermediate stages of the process to reveal the kinetics of the different processes.

Chlamydomonas reinhardtii is a suitable organism for studies of the photoactivation process since it can be grown in darkness without losing the ability to synthesize and assemble the components of PS II, except for the Mn cluster. When the cells are transferred to light, photoactivation will occur in 90% of the PS II centers with a half-time of less than 1 min over a broad light regime (*17*). The FUD 39 mutant strain of *C. reinhardtii* that lacks the 23 kDa extrinsic subunit of PS II is photoactivated in vivo but at a much slower rate, compared to the wild type, with a half-time of ≈5−6 min. The yield is also lower with about 70% of the centers being activated in the optimal case. The yield and the initial rate of photoactivation in the mutant are strongly dependent on the intensity of the activating light with a sharp optimum of the yield of activated centers around the very low light intensity of 1 μE m^{-2} s^{-1}. This suggests that the process is disturbed by photoinduced damaging reactions. The reason could be that the low affinity for Cl^- in this mutant hampered the assembly of functional Mn clusters. In this study, we have taken advantage of the slower photoactivation rate of the FUD 39 mutant to achieve higher resolution of the kinetics of the different parameters that change during the process.

We have used EPR spectroscopy and flash-induced variable fluorescence techniques to follow electron-transfer reactions and the status of the Mn cluster and Tyr_D in PS II during photoactivation. We found that the assembly of a functional Mn cluster is associated with increased electron-transfer rates on the acceptor side of PS II, indicating a close mechanistic and functional relationship between the two sides of the membrane-spanning protein complex. We also observed an effect on the less well-understood auxiliary electron donor Tyr_D during photoactivation, supporting the hypothesis that this compound serves a protective function in PS II when the Mn cluster is not functional.

It was also shown that, in this mutant, it is possible to resolve different kinetics of the events during photoactivation; those events clearly take place in a sequential way.

MATERIALS AND METHODS

Cell Growth and Photoactivation Conditions. FUD 39 mutant cells of *C. reinhardtii* were grown on Tris−acetate−phosphate medium (*18*) in complete darkness at 23 °C. The cells were taken to a light chamber after 3−5 days of growth when they were in early exponential growth phase, and no water splitting activity could be detected. Photoactivation was performed by illuminating the cells in the light chamber as described earlier (*17*). The cells were placed on ice and harvested immediately after the illumination was completed.

Thylakoid Membrane Preparation. Thylakoid membranes were prepared, immediately after the photoactivation treatment, as in (*19*). In the EPR samples, 1 mM EDTA was included in all buffers after the first washing step. The preparations were done in extremely weak green light (≈1 nE m^{-2} s^{-1}) at 0−4 °C, and the thylakoids were stored at −80 °C in 25 mM HEPES−NaOH, pH 7.0, 50 mM NaCl, and 400 mM sucrose (buffer A).

Electron-Transfer Measurements. Electron-transfer rates through PS II were measured spectroscopically as photoreduction of 2,6-dichlorophenolindophenol (DCPIP) at 590 nm, with or without the exogenous donor 2,2′-diphenylcarbonic dihydrazide (DPC) as in (*17*). DCPIP reduction rate was first measured in the absence of DPC which revealed centers active in water splitting. Thereafter, a new sample was measured in the presence of DPC. This resulted in an increased reduction rate of DCPIP due to electron transfer from PS II centers without a functional Mn cluster in addition to the active centers. We have defined the percentage of water splitting ability as the ratio between the reduction rate of DCPIP without exogenous donor and the reduction rate of DCPIP with the addition of exogenous donor.

Chlorophyll a Fluorescence Measurements. The decay of the flash-induced variable fluorescence yield in photoactivated and control samples was measured with a pulse-modulated fluorometer (Waltz Co., Effeltrich, Germany). Monitoring measuring light pulses (λ = 650 nm) were used at a frequency of 1.6 kHz. Single saturating actinic flashes (8 μs width at maximum) were provided by a Waltz XST-103 xenon flash lamp. Fluorescence detection began 120 μs after the flash. The measuring light was applied at a modulation amplitude of 100 kHz for the first 10 ms after the saturating flash. The thylakoid concentration was 20 μg of chlorophyll/mL in buffer A, and the final volume was 1.5 mL in a 3 mL glass fluorescence cuvette. Each sample was dark-adapted for 1 min before measurement. Data were collected and analyzed using the Q_A-FIP program, version 4.3 (Q_A-Data Oy, Turku, Finland). The curve fitting was done using free running parameters.

EPR Measurements. The prepared thylakoid suspensions were added to the EPR tubes in the dark without any additions and frozen at 77 K. The chlorophyll concentrations were on average 2 mg/mL. All EPR spectra were recorded at liquid He temperatures with a Bruker ESP380 X-band spectrometer equipped with an Oxford Instruments helium flow cryostat. Illuminations to induce the S_2 state were made at 200 K in an ethanol bath cooled with CO_2(s). Each sample was illuminated for 8 min in total. After illumination, the samples were immediately transferred to liquid nitrogen. Quantitative induction of the $Tyr_D^{\bullet}$ radical (signal II_{slow}) was achieved by thawing the samples to room temperature, illuminating them for 2 min at room temperature, and then allowing the samples to dark-adapt for 5 min before freezing in liquid nitrogen. All illuminations were done using heat-filtered white light from a 1000 W projector.

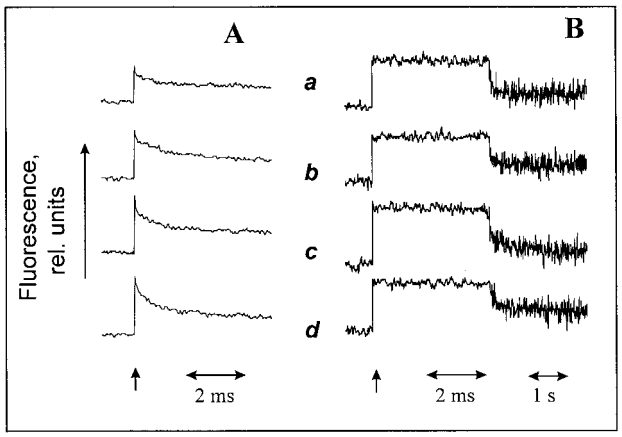

FIGURE 1: Effect of photoactivation on the decay kinetics of flash-induced variable fluorescence. After illumination of dark-grown cells at a light intensity of 0.8 μE m^{-2} s^{-1} for different periods of time, thylakoid membranes were prepared (Materials and Methods). The fluorescence yield, after single flashes, was measured in the absence (A) or in the presence (B) of 40 μM DCMU. Each trace shows the sum of 100 (A) or 10 (B) decay curves. The traces represent measurements in thylakoids from (a) dark-grown cells, (b and c) cells photoactivated for 2 and 60 min, respectively, and (d) light-grown cells. The flash is indicated by an arrow.

RESULTS

Modification of the Decay Kinetics of the Variable Fluorescence during Photoactivation. In dark-adapted samples, the primary electron acceptor Q_A is oxidized. The reduction of Q_A after a single flash gives rise to an increased fluorescence from PS II, the variable fluorescence (Fv), that decays as Q_A^- is reoxidized. The decay curve is composed of multiple kinetic phases. Forward electron transfer from Q_A^- depends on the redox state of Q_B. Q_B^- is formed with $t_{1/2} \approx 100-250$ μs, in thylakoids, while the formation of the hydroquinone occurs in 300−600 μs after the flash (*20, 21*). In some centers, at the moment of the flash, the Q_B site is empty and Q_B has to reoccupy the site before electron transfer from Q_A^- can occur. This is observed as a decay phase of Fv with $t_{1/2}$ of 5−15 ms (*20*−*22*).

If electron transfer from Q_A^- to Q_B is blocked (for example, in the presence of the herbicide DCMU), recombination reactions with donor side components will dominate. In intact PS II, Q_A^- recombines with the S_2 state (in dark-adapted samples) or the S_3 state on the time scale of seconds (*21*). In PS II with a perturbed water oxidizing center, due to lack of extrinsic subunits, cofactors, or Mn, recombination may occur with $Tyr_Z^\bullet$ in the millisecond time range (*23, 24*) or with P_{680}^+ in microseconds ($t_{1/2} \approx 50-150$ μs) (*25*−*27*).

Figure 1 shows the induction and decay of the variable fluorescence, after a single flash, in thylakoid membranes from dark-grown FUD 39 cells that have been photoactivated for 2 (trace b) or 60 (trace c) min with a light intensity of 0.8 μE m^{-2} s^{-1}. Under these conditions, maximal water oxidizing capacity, measured as the fraction of PS II centers that was able to photoreduce DCPIP, was reached after about 30 min of illumination (Figure 2A, squares).

Upon the flash, the detectable Fv was induced to an amplitude that was relativly small in the samples from the dark control and for the first 5 min of photoactivation. Fv was higher in samples activated for ≥10 min and in the light-grown control (Figure 1A, Table 1). Lower Fv in the samples with a diminished capacity of water splitting is probably explained by slower electron-transfer rates between Tyr_Z and P_{680}^+ when the Mn cluster is lacking. Without a functional Mn cluster, some of the Q_A^- formed instantaneously by the flash will recombine with P_{680}^+ on a time scale too fast to be resolved with our instrument, and, consequently, the amplitude of Fv would seem to be lower in those samples. In addition, any long-lived P_{680}^+ (due to slow electron donation from Tyr_Z) will also function as fluorescence quencher. It is thus likely that the increased amplitude of Fv with prolonged photoactivation time reflects the progressive activation of the Mn cluster.

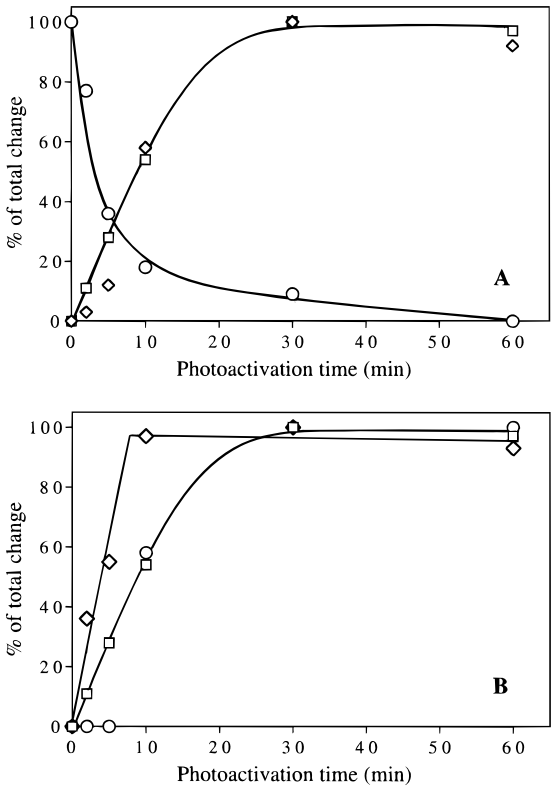

FIGURE 2: Correlation of various phenomena occurring during photoactivation. The changes in the indicated parameters are shown as a percentage of the total change occurring during the first 60 min of photoactivation. Dark-grown cells were treated as in Figure 1. Data are from Tables 1 and 2. Changes in (A) the water splitting ability (squares), $t_{1/2}$ of the fast decaying Fv phase in the presence of DCMU (recombination between Q_A^- and the donor side) (diamonds), and $t_{1/2}$ of the Fv millisecond decay phase in the absence of DCMU (forward electron transfer) (circles). Changes in (B) the water splitting ability (squares), the amplitude of the EPR signal II_{slow} (diamonds), and the amplitude of the EPR multiline signal (circles) as a function of photoactivation time.

The Fv decay curves could be fitted with two kinetic phases, one in the microsecond and the other in the millisecond time range (Figure 1A, Table 1). These phases disappeared in the presence of DCMU (Figure 1B), which blocks the electron transfer from Q_A^- to the Q_B site. Consequently, we assigned these kinetic phases to forward electron transfer. The rate of the fast phase was fairly constant with $t_{1/2} \approx 400$ μs. This is comparable with literature values for the Q_A^- to Q_B (Q_B^-) electron transfer, and the microsecond decay phase probably reflected a mix of these processes. The values in Table 1 seemingly indicate a slight decrease in $t_{1/2}$ of the fast phase during photoactivation even if the rates of the dark and light control were similar.

Table 1: Decay Kinetics of the Flash-Induced Variable Fluorescence Measured in Samples Photoactivated to a Varying Degree of Water Splitting Activity

time of preillumination[a] (min)	fraction of centers with functional Mn clusters[b,c] (%)	$t_{1/2}$ of Fv decay in absence of DCMU[c]		Fv/Fo in absence of DCMU[c]	$t_{1/2}$ of Fv decay in presence of DCMU[c]		Fv/Fo in presence of DCMU[c]
		μs (τ_1)	ms (τ_2)		ms	s	
0	0	390 (46)[d]	32 (54)[d]	0.33	90 (65)[d]	>10 (35)[d]	0.34
2	8	450 (47)	27 (53)	0.27	110 (60)	>10 (40)	0.28
5	18	430 (47)	18 (53)	0.28	170 (61)	>10 (39)	0.27
10	34	410 (54)	14 (46)	0.37	460 (53)	>10 (47)	0.34
30	62	370 (56)	12 (44)	0.35	720 (44)	>10 (56)	0.37
60	60	340 (54)	10 (46)	0.40	670 (54)	>10 (46)	0.48
light-grown	60	390 (54)	8 (46)	0.38	930 (53)	>10 (47)	0.41

[a] Illumination was performed at a light intensity of 0.8 μE m^{-2} s^{-1}. [b] The fraction of functional Mn clusters was determined by measuring the rate of light-induced electron transfer to DCPIP with and without the exogenous donor DPC as described under Materials and Methods. [c] Values are mean values from three different experiments (±10% for $t_{1/2}$ values). [d] Values in parentheses are the relative amplitudes (in percent of total Fv).

However, the changes are very small, only a factor of 1.3 between a sample photoactivated for 2 min and one photoactivated for 60 min. This probably lies within our experimental error, and we feel that our measurements reveal little or no change in the fast electron transfer from Q_A^- to the secondary electron acceptor.

The slower (millisecond) phase clearly changed during photoactivation. Beginning with a $t_{1/2}$ of 32 ms in the dark-grown control, the decay rate increased progressively and reached a $t_{1/2}$ of 10 ms in the sample photoactivated for 60 min (Table 1). This is similar to previously reported values for electron transfer from Q_A^- to an originally empty Q_B site (*20*−*22*). This suggests that the slow phase correlates to binding of Q_B to its site on PS II. It thus seems likely that the binding affinity of the secondary electron acceptor increases during the process of photoactivation. In Figure 2A, the change of the $t_{1/2}$ value normalized to a 0−100% scale is compared to the change in water splitting ability during an illumination period of 60 min. It shows that the enhanced electron-transfer rate from Q_A^- to the Q_B site, which probably reflects a change in binding affinity to the Q_B site, occurs earlier in the photoactivation process than the acquirement of water splitting ability.

In the presence of the herbicide DCMU (Figure 1B), the decay of Fv represents back-reactions from Q_A^- to oxidized components on the donor side of PS II. Also, here two phases could be resolved, one in the millisecond time range and a slower phase with a $t_{1/2}$ of more than 10 s. During photoactivation, the decay kinetics of the fast phase changed dramatically while the slow phase did not change (Table 1). The origin for the slow phase is unclear. In thylakoids from light-grown cells, the fraction of slowly decaying centers could represent inhibited centers that are unable to use water as electron donor. However, this is not the situation in dark-grown material. Instead, it is possible that the slow phase represents a perturbation of the PS II donor side induced by the lack of the 23 kDa extrinsic subunit in the mutant.

The fast decay phase is easier to assign. In thylakoids from dark-grown cells (Figure 1B, trace a), $t_{1/2}$ for the fast phase was about 90 ms. As the cells became photoactivated to a higher degree of water splitting activity, $t_{1/2}$ increased, and after 60 min photoactivation, it was about 700 ms (Table 1). In light-grown cells, where this phase mostly reflects $S_2Q_A^-$ recombination, $t_{1/2}$ was 10 times longer than in the dark-grown control, i.e., ≈900 ms.

The normal recombination partner of Q_A^- in a dark-adapted sample after a flash is the water oxidizing center in the S_2 state, and this recombination occurs normally in about 1 s in the presence of DCMU. In our samples, however, the water oxidizing center is expected to be absent in the dark-grown control and then to be successively built up during the process of photoactivation. Due to this, the recombination partner of Q_A^- is expected to change during photoactivation, and there are several possible candidates for this recombination partner. In dark-grown cells, it is likely that the principal recombination partner ($t_{1/2}$ ≈90 ms) is $Tyr_Z^\bullet$ and $Tyr_Z^\bullet Q_A^-$ recombination has been found to occur in this time regime in, e.g., NH_2OH-treated ($t_{1/2}$ ≈36 ms) or Tris-washed ($t_{1/2}$ ≈120 ms) PS II membranes (*23*, *24*, *28*).

The measurements of the flash induced fluorescence (Figure 1, Table 1) reveal changes in both the donor side and the acceptor side of PS II. A comparison of the changes in the $t_{1/2}$ values for the variable fluorescence decay phases and the fraction (in percent of total change) of centers able to split water is presented in Figure 2A. It seems clear that the slowdown of the Fv decay in the presence of DCMU (Figure 2A, diamonds) occurs on the same time scale as the activation of the water splitting activity (activation half-time ≈10 min). This can easily be understood since it indicates that the distance to the recombination partner increases at the same time as the water oxidizing center is built up during photoactivation. In contrast, those events that occur on the donor side of PS II are preceded by an increase in the rate of forward electron transfer from Q_A^- to the empty Q_B site as shown by the decreasing $t_{1/2}$ values of the millisecond decay phase in the absence of DCMU (Figure 2A, circles). This decrease occurs with a half-time of ≈3−4 min, which is significantly faster than the photoactivation of oxygen evolution. Thus, there is a possibility that the acceptor side of PS II is blocked by a diminished affinity of Q_B for its site in a dark-grown sample and that this block has to be overcome before the Mn cluster can begin to assemble.

EPR Spectroscopic Studies of Photoactivation. (i) Signal II_{slow} from $Tyr_D^\bullet$. A useful probe to the photochemistry in PS II is the redox state of TyrD. TyrD, that is identified as Tyr 160 on the D2 protein, is an auxiliary electron donor in PS II reaction centers. In a functional PS II reaction center, TyrD is readily oxidized by the Mn cluster in the S_2 or S_3 state upon illumination, forming a neutral radical that gives rise to a well-studied EPR spectrum, signal II_{slow}. The radical is stable for many hours in the dark (*29*) and decays by recombination with the Mn complex in the S_0 state (*30*). In the absence of the Mn cluster, TyrD is oxidized by $Tyr_Z^\bullet$,

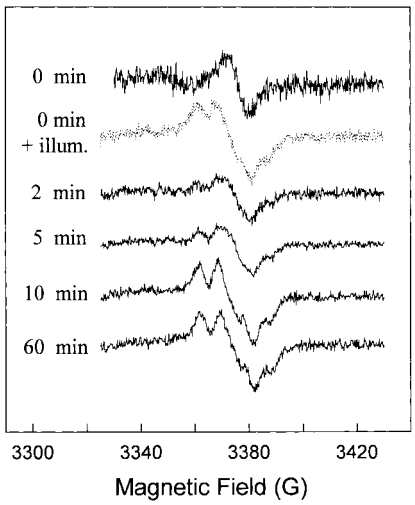

FIGURE 3: Induction of $Tyr_D^{\bullet}$ (signal II_{slow}) during photoactivation. Cells were treated as in Figure 1, and the EPR spectra of $Tyr_D^{\bullet}$ were recorded in the dark, in thylakoid membranes. Spectra are from cells photoactivated for the times indicated. The dashed trace shows the maximal signal II_{slow} induced after illumination at room temperature of the nonactivated control. EPR conditions: $T = 20$ K; microwave power, 1.83 μW; microwave frequency, 9.45 GHz; modulation amplitude, 4 G; modulation frequency, 100 kHz.

Table 2: EPR Signals Measured in Thylakoid Membranes from Photoactivated and Control Cells

time of illumination (min)[a]	amplitude of $Tyr_D^{\bullet}$ (signal II_{slow}) (%)[b]	amplitude of multiline signal (%)[b]
0	6	0
2	40	0
5	58	0
10	97	41
30	100	nd[c]
60	93	71
light-grown	83	100

[a] Illumination was performed at a light intensity of 0.8 μE m^{-2} s^{-1}. [b] Amplitudes are given in percent of maximal signal and are corrected for varying chlorophyll concentrations. The signal size of $Tyr_D^{\bullet}$ (signal II_{slow}) was determined by double integration of the radical and the amplitude of the S_2 state ML signal by adding the amplitudes of the three peaks marked in Figure 4. [c] nd, not determined.

and it decays in a pH-dependent manner within tens of minutes to a few hours (*31*).

As Tyr_D oxidation demands light, signal II_{slow} is not observed in PS II from dark-grown cells (Figure 3; 0 min). Instead, we observe a small radical signal of unknown origin which does not originate from the photosystems (no light has been applied to the sample). Progressive photoactivation of the cells resulted in oxidation of Tyr_D observable as an increase in the size of signal II_{slow} (Figure 3; 2−60 min). After only 10 min of photoactivation (reaching about 55% of maximal water splitting capacity, Figure 2), Tyr_D was oxidized in all PS II centers, and further photoactivation did not result in any further increase of the signal (Figure 3, Table 2). It is, however, important to note that when the samples were subjected to further illumination in the EPR tubes at room temperature, Tyr_D could be oxidized in all PS II centers in all samples, i.e., to the same level as in the sample photoactivated for 10 min (Figure 3; dashed spectrum). Consequently, it is possible to oxidize Tyr_D in all centers, but during photoactivation, the maximal level is not reached before 10 min of illumination.

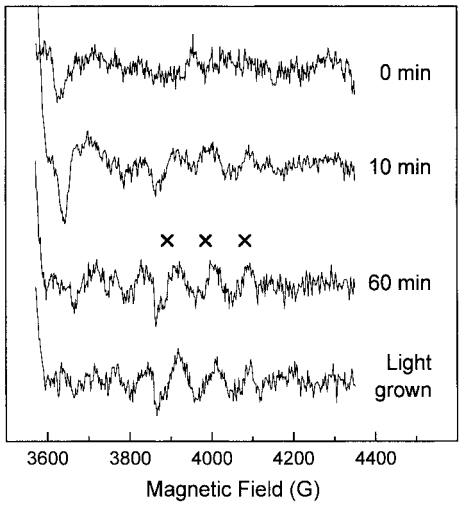

FIGURE 4: Partial EPR spectra of the S_2-state multiline EPR signal induced in samples photoactivated for the indicated times and prepared as in Figure 1. The spectral amplitudes have been normalized to account for varying chlorophyll concentrations. The figure shows the high-field part ($g > 2$) of the multiline EPR signal. The crosses indicate the peaks used for determination of the signal amplitude (Table 2). (The low-field part is less clear due to overlapping EPR signals from other components in the thylakoid membrane.) EPR conditions: $T = 10$ K; microwave power, 18 mW; microwave frequency, 9.44 GHz; modulation amplitude, 20 G; modulation frequency, 100 kHz.

The amount of $Tyr_D^{\bullet}$ induced by photoactivation reached a half-maximum after about 5 min (Figure 2B). This is similar to the half-time of the increase in forward electron transfer between the Q_A and the Q_B sites (Figure 2A, circles; and Figure 2B, diamonds) and, most importantly, clearly faster than the activation of the water oxidizing capacity (Figure 2B, squares).

(ii) The S_2 State Multiline Signal. In the S_2 state, the Mn cluster in the oxygen evolving complex gives rise to the so-called S_2 state multiline EPR signal. This complex EPR signal, which is observable at low temperatures, is indicative of an intact functional Mn cluster. The multiline signal has never been observed in PS II preparations with a perturbed or nonfunctional Mn cluster. Here, we have studied the assembly of a functional Mn cluster during photoactivation by following the appearance of the multiline signal.

PS II from dark-grown cells does not contain functional Mn clusters, and no water splitting activity was detected (Table 1). Consequently, no S_2 multiline signal could be detected in those samples (Figure 4). Photoactivation of the dark-grown cells for 10 min induced the S_2 multiline signal in a fraction of the centers, and after 60 min of illumination, when maximal water splitting ability was reached, the amplitude of the S_2 multiline signal was 71% of the light-grown control (Figure 4, Table 2). We could not detect any multiline signal in samples photoactivated for shorter times that 10 min, but the potential signal amplitude from complete manganese clusters was probably below the noise level in this case.

This increase in amplitude of the S_2 multiline signal occurred in parallel with the acquirement of water splitting ability (Figure 2B). This was expected since the multiline signal emanates from a functional tetrameric Mn cluster. Thus, both the increase of the S_2 multiline signal and the decreasing decay rate of the variable fluorescence phase,

attributed to back-reaction with the donor side, coincided with the increasing rate of water splitting (Figure 2A,B). This strengthens the hypothesis that those three assays reflect the assembly of a functional Mn cluster and that this process occurs with a half-time of about 10 min under our conditions.

DISCUSSION

The sequential stepwise reactions that occur on the donor side of PS II during photoactivation of the Mn cluster have been much studied, and in essence, the binding of the first two Mn ions occurs in photoreactions that involve two photoacts with a defined intervening dark period. Thereafter, the entire Mn cluster is assembled in a series of reactions that do not require light. In contrast to this detailed knowledge, there is little information of how the photoactivation of the Mn cluster influences the function of other redox components and electron-transfer reactions in PS II. Here, we have measured parameters outside the Mn cluster in PS II during the course of photoactivation to get more insight into the complexity of this process.

We have used the FUD 39 mutant, mainly because its slower photoactivation rate allows easier resolution of the kinetics of the different events during photoactivation. By using a mutant, there is a possibility that the observed sequence of events leading to photoactivation cannot be extrapolated to the wild-type situation. To minimize this risk, we have chosen a light regime when activating the cells, which is optimal both in the mutant and in the wild type. Furthermore, in the FUD 39 mutant, our protocol results in the highest possible yield of active centers, hence minimizing any photoinhibiting reactions. Thus, we believe that most of our results are relevant also for PS II from the wild type.

A potential danger for a developing PS II is that it absorbs light energy and produces charge separations before a functional Mn cluster is assembled. The assembling PS II center might thus be vulnerable to donor side induced photoinhibition which is a serious situation that might lead to degradation of the D1 protein (*32, 33*). In accordance with this, it has been shown (*17*) that the donor side mutant, FUD 39, with suppressed efficiency in oxygen evolution and photoactivation rate was very susceptible to light-induced damage during photoactivation. Alternative pathways for rereduction of the highly oxidizing species $Tyr_Z^{\bullet}$ and P_{680}^{+} are supposed to exist to avoid photoinhibition during photoactivation. There are in principle two ways to rereduce the donor side of PS II in the absence of a functional Mn cluster: (i) forward electron-transfer reactions of the acceptor side can be blocked, resulting in increased charge recombination with the donor side; (ii) an alternative donor can reduce P_{680}^{+} or $Tyr_Z^{\bullet}$ temporarily or by participating in cyclic electron flow in PS II.

An acceptor side block has been proposed by Johnson et al. (*34*), who showed that the midpoint potential of Q_A changed from +110 mV to −80 mV upon photoactivation, thus promoting forward electron transfer. Here, we measured the reoxidation of Q_A^- after single flashes in order to study the kinetics of electron transfer from Q_A^- to Q_B (Q_B^-). If inhibition of the electron-transfer reactions on the acceptor side exists, we expected this to be seen as slower kinetics of the Q_A^- reoxidation in the dark-grown control and in early phases of photoactivation.

We observed two kinetics of the decay of Q_A^- after single flashes, one (τ_1) in the microsecond and the other (τ_2) in the millisecond time range (Table 1). According to the $t_{1/2}$ value of about 400 μs, τ_1 most probably reflects electron transfer from Q_A^- to Q_B (Q_B^-) (*20, 21*). There was indeed a change in τ_1 during photoactivation (Table 1), but the differences are small, and we conclude that there is no significant effect on the Q_A^- to Q_B (Q_B^-) electron-transfer rates during photoactivation under our conditions.

Interestingly, there was a significant change in the millisecond rate constant, τ_2, during the course of photoactivation. The $t_{1/2}$ value, which was 32 ms in the dark-grown control and 8 ms in the light-grown control, attributed this phase to electron transfer from Q_A^- to Q_B in those centers where the Q_B site has to be reoccupied prior to reoxidation of Q_A^- (*20*−*22*). Another possibility might be that this phase reflects back-reaction with the donor side. This was, however, excluded since (i) this phase could not be seen in the presence of DCMU (Table 1) and (ii) the addition of the electron donor DPC did not change the kinetics of this phase (not shown).

If we accept that τ_2 reflects electron transfer from Q_A^- to Q_B in a site where Q_B has to bind prior to electron transfer, then the decrease in τ_2 with photoactivation might indicate an increased binding efficiency of Q_B to its site in PS II. The most likely explanation is that PS II undergoes a conformational change during photoactivation. Since both the Q_B site and most of the Mn binding ligands are believed to reside on the same subunit, the D1 protein, it seems possible that the binding of the Mn ions triggers a conformational change on the acceptor side. Here it should be pointed out that the slight increase in amplitude of the microsecond decay of Q_A^- [i.e., Q_A^- to Q_B (Q_B^-) in the site] that we observe during photoactivation (Table 1) also indicate increased binding of Q_B.

Interestingly, the Mn cluster did not assemble to a functional unit before the change at the acceptor side had occurred [deduced from comparison of the change in τ_2 with the change in water splitting activity (Figure 2A)]. Thus, it is likely that early events in the photoactivation process (like binding of the first Mn ion) trigger an opening of the electron transfer out from PS II which in turn could be a prerequisite for further events in the process. Thus, blocking of the acceptor side can be an important way to avoid photoinhibition in centers without a Mn cluster, but this block is released very early during photoactivation.

With a decreased rate of electron transfer between Q_A^- and the Q_B site, the recombination frequency between Q_A^- and the donor side will increase. Such a situation might dominate in the beginning of photoactivation (see above). Thus, during illumination the charge separation pair $Tyr_Z^{\bullet}Q_A^-$ is continuously forming and recombining. However, there exist alternative donors which might reduce $Tyr_Z^{\bullet}$ or P_{680}^{+}. Tyr_D can produce stable charge separations in a PS II center lacking a functional Mn cluster and has been shown to be photooxidized by P_{680}^{+} under various circumstances (*24, 31*).

We observed an accumulation of $Tyr_D^{\bullet}$ during the first 10 min of photoactivation (Figure 2B). The rate at which $Tyr_D^{\bullet}$ was formed coincided with the increased electron-transfer rate on the acceptor side ($t_{1/2} \approx 5$ min) (Figure 2A,B). This result indicates that the observed electron transfer (Q_A^- decay in the millisecond time range, Figures 1 and 2) really is a

forward reaction that calls for an auxiliary electron donor to reduce $Tyr_Z^{\bullet}/P_{680}^{+}$ before the Mn cluster is functional. When the electron transfer from Q_A^- to Q_B becomes more effective, but the Mn cluster is incompetent, Tyr_D might reduce P_{680}^{+}. This is a low quantum yield process (*24*) but will nevertheless relieve the oxidative stress from long-lived P_{680}^{+} or $Tyr_Z^{\bullet}$. Thus, Tyr_D can function to protect PS II against photodamage during early phases of photoactivation. Since all PS II centers are born without a functional Mn cluster, there is always a need for a protective donor. This might be one explanation for the existence of Tyr_D despite its slow and seemingly inefficient electron transfer to P_{680}^{+}.

To summarize, the photoactivation process in the FUD 39 mutant seems to take place in a stepwise fashion. Early in the process some presently unidentified event(s), e.g., the binding of the first Mn ion(s) trigger(s) what is probably a conformational change on the acceptor side of PS II which enhances the binding affinity for the secondary plastoquinone acceptor, Q_B. This increase in the electron-transfer rate to Q_B clearly occurs before the water oxidizing center is functional. Together with the improved forward electron transfer from Q_A^-, this explains the increase in net oxidation of the auxiliary electron donor Tyr_D which occurs concomitant with the opening of the acceptor side. Finally, when the water oxidizing center is functional, forward electron transfer from Q_A^- is efficient, and recombination reactions from Q_A^- to $Tyr_Z^{\bullet}$ are absent.

REFERENCES

1. Andersson, B., and Franzén, L.-G. (1992) in *New Comprehensive Biochemistry: Molecular Mechanisms in Bioenergetics* (Ernster, L., Ed.) Vol. 23, pp 121−143, Elsevier Science Publishers B. V, Amsterdam.
2. Vermaas, W., Styring, S., Schröder, W., and Andersson, B. (1993) *Photosynth. Res. 38*, 249−263.
3. Debus, R. J. (1992) *Biochim. Biophys. Acta 1102*, 269−352.
4. Rutherford, A. W., Zimmerman, J.-L., and Boussac, A. (1992) in *The Photosystems: Structure, Function and Molecular Biology* (Barber, J., Ed.) Vol. 11, pp 179−229, Elsevier, Amsterdam.
5. Cheniae, G. M., and Martin, I. F. (1971) *Biochim. Biophys. Acta 253*, 153−166.
6. Ono, T., and Inoue, Y. (1987) *Plant Cell Physiol. 28(7)*, 1293−1299.
7. Tamura, N., and Cheniae, G. (1987) *Biochim. Biophys. Acta 890*, 179−194.
8. Miller, A.-F., and Brudvig, G. W. (1990) *Biochemistry 29*, 1385−1392.
9. Boussac, A., Maison-Peteri, B., Etienne, A.-L., and Vernotte, C. (1985) *Biochim. Biophys. Acta 808*, 231−234.
10. Yamashita, T., and Ashizawa, A. (1985) *Arch. Biochem. Biophys. 238(2)*, 549−557.
11. Miller, A.-F., and Brudvig, G. W. (1989) *Biochemistry 28*, 8181−8190.
12. Miyao, M., and Inoue, Y. (1991) *Biochemistry 30*, 5379−5387.
13. Andersson, B., Salter, A. H., Virgin, I., Vass, I., and Styring, S. (1992) *J. Photochem. Photobiol. B: Biol. 15*, 15−31.
14. Prasil, O., Adir, N., and Ohad, I. (1992) in *The Photosystems: Structure, Function and Molecular Biology* (Barber, J., Ed.) Elsevier, Amsterdam.
15. Styring, S., and Jegerschöld, C. (1994) in *Photoinhibition of Photosynthesis; from Molecular Mechanisms to the Field* (Baker, N. R., and Bowyer, J. R., Eds.) pp 51−73, BIOS Scientific Publishers, Oxford.
16. Thompson, L. K., and Brudvig, G. W. (1988) *Biochemistry 27*, 6653−6658.
17. Rova, M., McEwen, B., Fredriksson, P.-O., and Styring, S. (1996) *J. Biol. Chem. 271*, 28918−28924.
18. Harris, E. H. (1989) *The Chlamydomonas Sourcebook: A Comprehensive Guide to Biology and Laboratory Use*, Academic Press, San Diego.
19. Rova, M., Franzén, L.-G., Fredriksson, P.-O., and Styring, S. (1994) *Photosynth. Res. 39*, 75−83.
20. Crofts, A. R., and Wraight, C. A. (1983) *Biochim. Biophys. Acta 726*, 149−185.
21. Renger, G., Eckert, H.-J., Bergmann, A., Bernarding, J., Liu, B., Napiwotzki, A., Reifarth, F., and Eichler, H. J. (1995) *Aust. J. Plant Physiol. 22*, 167−181.
22. Vass, I., Styring, S., Hundal, T., Koivuniemi, A., Aro, E.-M., and Andersson, B. (1992) *Proc. Natl. Acad. Sci. U.S.A. 89*, 1408−1412.
23. Yerkes, C. T., Babcock, G. T., and Crofts, A. R. (1983) *FEBS Lett. 158*, 359−363.
24. Buser, C. A., Thompson, L. K., Diner, B. A., and Brudvig, G. W. (1990) *Biochemistry 29*, 8977−8985.
25. Conjeaud, H., Mathis, P., and Paillotin, G. (1979) *Biochim. Biophys. Acta 546*, 280−291.
26. Ono, T., Conjeaud, H., Gleiter, H., Inoue, Y., and Mathis, P. (1986) *FEBS Lett. 203*, 215−219.
27. Rutherford, A. W. (1988) in *Light-Energy Transduction in Photosynthesis: Higher Plant and Bacterial Models* (Stevens, S. E. J., and Bryant, D. A., Eds.) pp 163−177, The American Society of Plant Physiologists, Rockville, MD.
28. Dekker, J. P., van Gorkom, H. J., Brok, M., and Ouwehand, L. (1984) *Biochim. Biophys. Acta 764*, 301−309.
29. Babcock, G. T., and Sauer, K. (1973) *Biochim. Biophys. Acta 325*, 483−503.
30. Styring, S., and Rutherford, A. W. (1987) *Biochemistry 26*, 2401−2405.
31. Vass, I., and Styring, S. (1991) *Biochemistry 30*, 830−839.
32. Aro, E.-M., Virgin, I., and Andersson, B. (1993) *Biochim. Biophys. Acta 1143*, 113−134.
33. Jegerschöld, C., Virgin, I., and Styring, S. (1990) *Biochemistry 29*, 6179−6186.
34. Johnson, G. N., Rutherford, A. W., and Krieger, A. (1995) *Biochim. Biophys. Acta 1229*, 202−207.

BI980381H